JOURNAL OF MAGNETIC RESONANCE IMAGING 37:566–575 (2013)

Review

MRI Evaluation of Acute Appendicitis in Pregnancy

CME

Catherine Dewhurst, MD,[1] Peter Beddy, MD,[2] and Ivan Pedrosa, MD[3]*

This article is accredited as a journal-based CME activity. If you wish to receive credit for this activity, please refer to the website: www.wileyhealthlearning.com

ACCREDITATION AND DESIGNATION STATEMENT

Blackwell Futura Media Services designates this journal-based CME activity for a maximum of 1 *AMA PRA Category 1 Credit*™. Physicians should only claim credit commensurate with the extent of their participation in the activity.

Blackwell Futura Media Services is accredited by the Accreditation Council for Continuing Medical Education to provide continuing medical education for physicians.

EDUCATIONAL OBJECTIVES

Upon completion of this educational activity, participants will be better able to discuss a comprehensive MRI protocol for evaluation of pregnant women with abdominal pain.

ACTIVITY DISCLOSURES

No commercial support has been accepted related to the development or publication of this activity.

Faculty Disclosures:

The following contributors have no conflicts of interest to disclose:

Editor-in-Chief: C. Leon Partain, MD, PhD

CME Editor: Scott B. Reeder, MD, PhD

CME Committee: Scott Nagle, MD, PhD, Pratik Mukherjee, MD, PhD, Shreyas Vasanawala, MD, PhD, Bonnie Joe, MD, PhD, Tim Leiner, MD, PhD, Sabine Weckbach, MD, Frank Korosec, PhD

Authors: Catherine Dewhurst, MD, Peter Beddy, MD, and Ivan Pedrosa, MD

This manuscript underwent peer review in line with the standards of editorial integrity and publication ethics maintained by *Journal of Magnetic Resonance Imaging*. The peer reviewers have no relevant financial relationships. The peer review process for *Journal of Magnetic Resonance Imaging* is double-blinded. As such, the identities of the reviewers are not disclosed in line with the standard accepted practices of medical journal peer review.

Conflicts of interest have been identified and resolved in accordance with Blackwell Futura Media Services's Policy on Activity Disclosure and Conflict of Interest. No relevant financial relationships exist for any individual in control of the content and therefore there were no conflicts to resolve.

INSTRUCTIONS ON RECEIVING CREDIT

For information on applicability and acceptance of CME credit for this activity, please consult your professional licensing board.

This activity is designed to be completed within an hour; physicians should claim only those credits that reflect the time actually spent in the activity. To successfully earn credit, participants must complete the activity during the valid credit period.

Follow these steps to earn credit:

- Log on to www.wileyhealthlearning.com
- Read the target audience, educational objectives, and activity disclosures.
- Read the article in print or online format.
- Reflect on the article.
- Access the CME Exam, and choose the best answer to each question.
- Complete the required evaluation component of the activity.

This activity will be available for CME credit for twelve months following its publication date. At that time, it will be reviewed and potentially updated and extended for an additional period.

[1]Beth Israel Deaconess Medical Center, Boston, Massachusetts, USA.
[2]St James's Hospital and Trinity College, Dublin, Ireland.
[3]University of Texas Southwestern Medical Center, Dallas, Texas, USA.
*Address reprint requests to: I.P., Department of Radiology, University of Texas Southwestern Medical Center, 5323 Harry Hines Blvd., Dallas, TX 75390. E-mail: ivan.pedrosa@UTSouthwestern.edu
Received January 24, 2012; Accepted June 29, 2012.
DOI 10.1002/jmri.23765
View this article online at wileyonlinelibrary.com.

In recent years, magnetic resonance imaging (MRI) has become a valuable diagnostic tool for evaluation of acute abdominal pain in pregnancy. MRI offers an opportunity to identify the normal or inflamed appendix as well as a variety of other pathologic conditions that can masquerade clinically as acute appendicitis in pregnant women. Visualization of the normal appendix by MRI virtually excludes the diagnosis of acute appendicitis and may help reduce the negative laparotomy rate in this patient population. Here we discuss a comprehensive MRI protocol for evaluation of pregnant women with abdominal pain, focusing on the appearance and location of the normal and diseased appendix, and we describe an approach to diagnosing acute appendicitis and other conditions with MRI.

Key Words: MRI; appendicitis; pregnancy
J. Magn. Reson. Imaging 2013;37:566–575.

ACUTE APPENDICITIS occurs in ~1 in 1400 to 1 in 6600 pregnancies and is the most common cause of abdominal pain in pregnancy requiring surgery (1–4). The clinical diagnosis of appendicitis is more challenging, as the clinical examination and laboratory tests are often unhelpful due to the normal anatomical and physiological alterations that occur during pregnancy (5). The differential diagnosis is wide, ranging from obstetric, gynecologic, to other abdominal pathologies such as renal colic. Diagnostic imaging with ultrasound (US) can be limited due to the changes in body habitus and computed tomography (CT) is not desirable due to the radiation dose to the fetus (6,7). Delay in diagnosis may result in significant risk to the fetus, with a fetal mortality of up to 35%–55% reported in patients with perforated appendicitis versus 1.5% for a nonruptured appendix (8,9). Maternal morbidity is also reduced if the appendix is intact at the time of surgery.

Magnetic resonance imaging (MRI) has only recently become a relatively common investigation for acute abdominal pain in pregnancy (10–13). US is performed initially due to its low cost and availability, although its efficacy is reduced by technical difficulties from poor penetration from increased abdominal girth (14,15). The multiplanar capacity of MRI and excellent soft tissue contrast coupled with the lack of ionizing radiation makes it the optimal test for acute appendicitis if the appendix is not visualized with US. This article reviews a comprehensive MRI protocol for evaluation of the pregnant abdomen, highlights the appearance and location of the normal and diseased appendix, and describes an approach to diagnosing acute appendicitis with MRI.

MRI TECHNIQUE

The American College of Radiologists has indicated that pregnant patients should undergo MRI evaluation, irrespective of the gestational age, when MRI represents the only means for obtaining the diagnosis and the results of the study have the potential to affect the patient's management (16). In the authors' institutions, written informed consent is obtained from all patients before the MRI examination. Patients receive an oral contrast preparation containing 450 mL of ferumoxsil (Gastromark; Mallinckrodt Medical, St. Louis, MO) combined with 300 mL of barium sulfate (Readi-Cat 2; E-Z-Em, Westbury, NY) 1.5 hours before the MRI study. The oral preparation acts as a negative contrast agent (ie, dark signal) on both T1- and T2-weighted imaging sequences without causing considerable susceptibility artifact. Several authors have proposed a nonoral contrast technique with good

Table 1
MRI Protocol for Pregnant Patients With Suspected Appendicitis

	Coronal single-shot FSE	Axial single-shot FSE	Sagittal single-shot FSE	Axial 2D FS single-shot FSE	IP and OP 2D T1W GRE	2D TOF	DWI
Sequence type	Single shot	Single shot	Single shot	Single shot	GRE	GRE	
Repetition time (msec)	800–1100	800–1100	800–1100	800–1100	205	30.0	10,000
Echo time (msec)	60	60	60	60	2.2/4.5	60	60–85
Flip Angle (degrees)	130–155	130–155	130–155	130–155	80	45	
2D or 3D	2D	2D	2D	2D	2D	2D	2D
Section thickness (mm)	4	4	4	4	5	3	5
Gap (mm)	1	1	1	1	2	1	0
Field of View (mm)	350	350	350	350	350	350	320
Number of partitions or Sections	20	20	20	20	32	24	48
Orientation	Coronal	Axial	Sagittal	Axial	Axial	Axial	Axial
Phase x frequency steps	192x256	192x256	192x256	192x256	160x256	128x256	64x64
Rectangular Field of View	No	0.75	0.75	0.75	0.75	0.75	0.75
Fat Suppression	No	No	No	Yes	No	No	Yes
Single or multiple shots	Single	Single	Single	Single	Multiple	Multiple	Single
Bandwidth (kHz)[b]	62.5	62.5	62.5	62.5	62.5	31.25	
Breathold	Yes	Yes	Yes	Yes	Yes	Yes	Yes
b-value (sec/mm2)							850–1000

[a]FSE, fast spin echo; FS, fat-saturated; IP, in-phase; OP, opposed phase; T1W, T1 weighted; GRE, gradient echo; TOF, time of flight; DWI, diffusion weighted imaging.
[b]62.5 kHz = 488 Hz/pixel, 31.25 kHz = 244 Hz/pixel.

Figure 1. Coronal SSFSE T2-weighted imaging of a 26-year-old woman at 7 weeks gestational age and abdominal pain demonstrating a normal appendix (arrow) measuring less than 6 mm in diameter and without appreciable intraluminal fluid.

results (ie, similar sensitivity and specificity as that of those using oral contrast), although these focused primarily on the diagnostic accuracy of MRI (12,17–19). The oral contrast may be an invaluable component of the examination, however, as it increases the confidence in visualizing the normal appendix and possibly affects surgical outcomes by avoiding unnecessary laparotomies (20). Reports about the impact of MRI on surgical outcomes using an MRI protocol without oral contrast are lacking at the moment. Intravenous gadolinium-based contrast agents are not administered, as they have been shown to cross the placenta, and the long-term consequences of gadolinium exposure to the fetus are unknown (21). We perform MRI examinations on a 1.5-T system with the patient in the supine position and with a multichannel body phased-array coil (12–16 elements). The parameters of the sequences employed are detailed in Table 1. All MRI studies are monitored by a radiologist to ensure appropriate anatomic coverage. Furthermore, if the oral contrast has not reached the cecum at this point, the patient may be reimaged after a short time interval to allow the contrast to progress into the colon if needed. All sequences in the study are performed during suspended end expiration lasting up to 20 seconds. Total imaging time is ~30 minutes.

The T2-weighted half-Fourier single-shot fast spin-echo (SSFSE) images are initially assessed for anatomic localization of the appendix in the axial, sagittal, and coronal plane. In addition, axial SSFSE images are obtained using frequency-selective fat saturation to better identify regions of edema, inflammation, and fluid. The half-Fourier strategy provides the opportunity for very fast SSFSE acquisitions, with each image obtained in ~1 second. Moreover, because SSFSE images are acquired sequentially, they are relatively motion-insensitive compared to standard spin echo T2-weighted imaging. Limited maternal breathholding capacity and fetal motion are particular problems encountered in MRI in pregnancy and the SSFSE sequences perform reliably in this clinical setting (22,23).

Transverse 2D time-of-flight (TOF) T2*-weighted gradient-echo images are used to differentiate the appendix from distended pelvic and retroperitoneal vessels, which can easily simulate the appendix on SSFSE imaging (23). In addition, these images can help confirm the presence of air and/or oral contrast in the lumen of the appendix (see Normal Appendix, below), both of which indicate the absence of acute inflammation.

Axial T1-weighted in-phase and opposed-phase gradient echo (GRE) imaging is helpful in characterizing soft tissue lesions by allowing one to differentiate

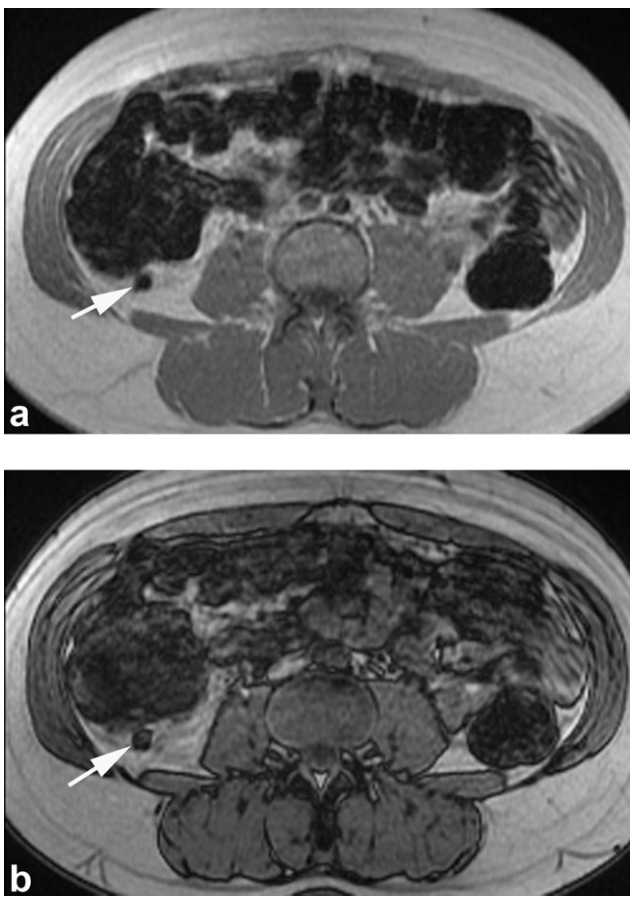

Figure 2. A 21-year-old woman at 15 weeks gestational age with right lower quadrant pain. Axial in-phase **(a)** image shows blooming of the normal appendix (arrow) compared with the out-of-phase image **(b,** arrow), indicating the presence of air and/or oral contrast in its lumen.

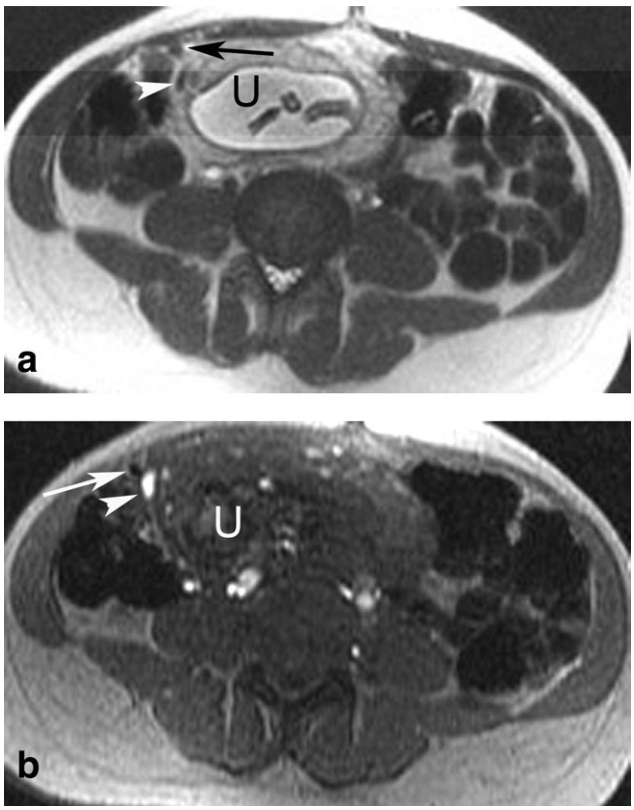

Figure 3. A 41-year-old woman at 18 weeks gestational age with right lower quadrant pain. Axial T2-weighted SSFSE image **(a)** shows two hypointense tubular structures in the anterior abdomen adjacent to the gravid uterus (U). Axial T2*-weighted gradient-echo images (b) at the same level demonstrates flow within the posterior structure (arrowhead), which represents a venous collateral of the gonadal vein. Note the blooming (ie, low signal intensity) of the normal appendix (arrow) owing to the presence of air and/or negative oral contrast agent in its lumen.

lipid, hemorrhagic, and proteinaceous content. Additionally, these sequences can identify areas of magnetic susceptibility, such as air, hemosiderin, or calcium (22,23).

Diffusion-weighted MRI (DWI) with quantitative measurements of apparent diffusion coefficient (ADC) values is an increasingly applied technique in abdominal imaging due to its ability to depict areas of inflammation and characterize neoplastic lesions without the need for intravenous contrast administration (24,25). DWI has shown potential in the evaluation of acute appendicitis (26); however, to our knowledge, its use has not been systematically studied in pregnancy. The authors use a respiratory triggered, axial, single-shot echo-planar diffusion-weighted sequence with B-values of 0 and 850 sec/mm^2. Fat saturation strategies, including frequency selective pulses and inversion recovery techniques, are helpful to improve saturation of background signal and detection of pathologic processes. Respiratory triggering improves anatomic coregistration and minimizes artifacts related to respiratory motion. However, the use of respiratory bellows can be challenging, especially in the third trimester, as the gravid uterus may result in shallow respiration, which may not trigger the image acquisition (27,28).

NORMAL APPENDIX

The normal appendix is a blind-ending tubular structure arising 1–3 cm inferior to the ileocecal valve at the medial aspect of the cecum (29). It measures an average of 10 cm in length, and has a wall thickness of 2 mm. The appendix is considered normal when its diameter is equal to or less than 6 mm and/or it is filled with oral contrast material, air, or both (Fig. 1). Both air and oral contrast within the normal appendix are of low signal intensity on T1- and T2-weighted images and become more prominent on T2*-weighted images (TOF and T1-weighted GRE images) due to the blooming effect from magnetic susceptibility (13,30). Because the blooming effect increases proportionally to the echo time (TE), it is more pronounced on the TOF images than that of the GRE images in our protocol; and, in the latter, the blooming effect is similarly more evident on the in-phase images than the

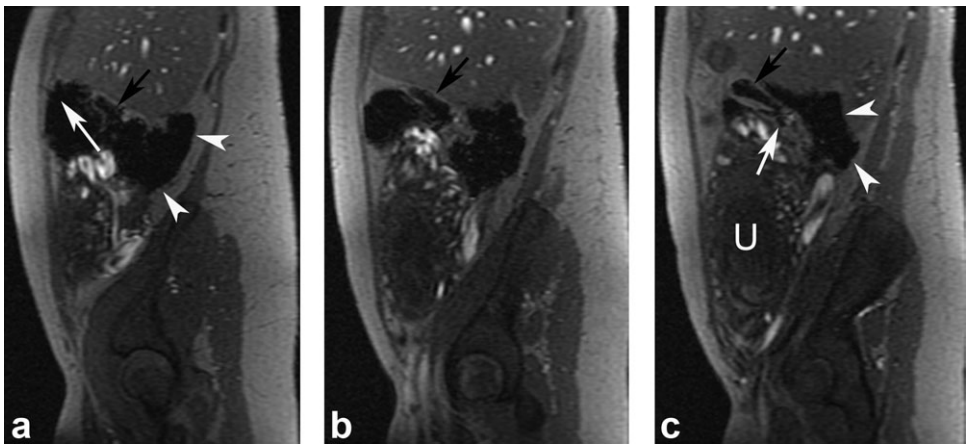

Figure 4. Contiguous time-of-flight T2*-weighted gradient echo images of a 21-year-old woman at 31 weeks gestational age acquired sagittally through the cecum in this patient for better demonstration of the anatomy. Note anterior tilting of the cecum (white arrow in **a)** and elevation of the terminal ileum (black arrow in **a–c)** relative to the normally oriented ascending colon (white arrowheads). The appendix (white arrow in c) is demonstrated in an elevated location due to displacement of the normal anatomy by the gravid uterus (U).

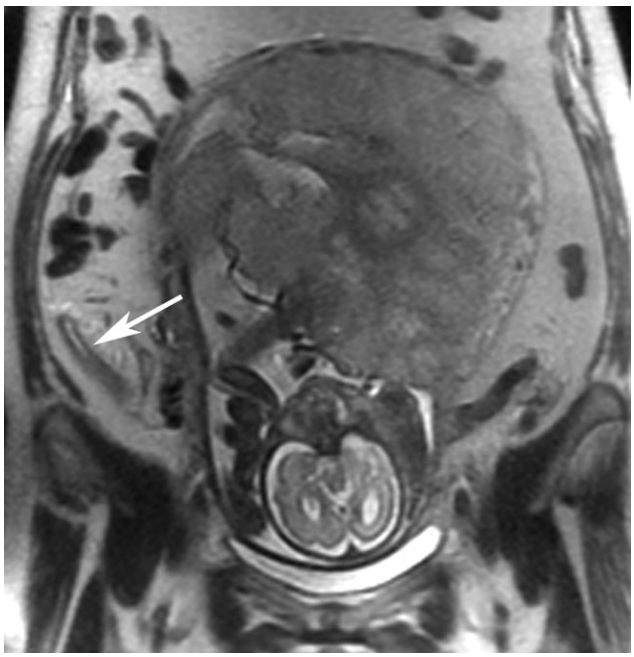

Figure 5. Coronal SSFSE T2-weighted imaging of a 41-year-old woman with a twin pregnancy at 26 weeks gestational age and right-sided abdominal pain demonstrates an inflamed appendix containing intraluminal fluid that is bright on T2-weighted imaging (arrow). Findings are consistent with acute appendicitis, which was confirmed after appendectomy.

opposed-phase images (Fig. 2a,b). In the absence of oral contrast, the normal appendix is seen as a cord-like structure of intermediate signal intensity, similar to that of the bowel wall (29). Dilated retroperitoneal and pelvic veins, in particular the gonadal veins during the second and third trimester, can simulate the normal appendix on SSFSE sequences. Flow within the vessels on axial TOF T2*-weighted GRE images is useful in differentiating the appendix from vessels (Fig. 3) (28).

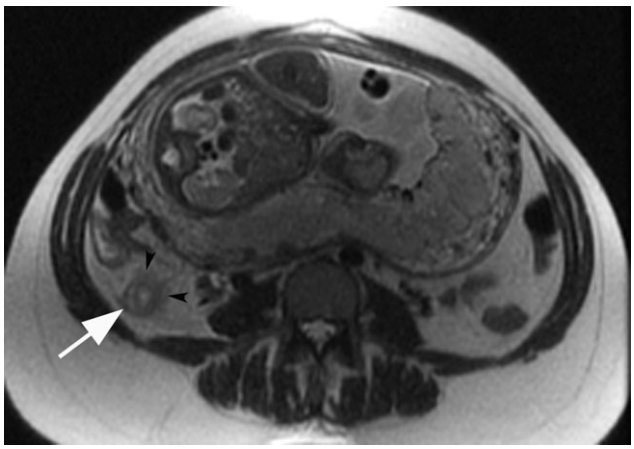

Figure 6. Axial SSFSE T2-weighted imaging of a 21-year-old woman at 30 weeks gestational age with right lower quadrant pain demonstrating a thick walled appendix with high signal intensity in the lumen (arrow) and periappendiceal fat stranding (arrowheads). Uncomplicated acute appendicitis was confirmed at surgery and histopathology.

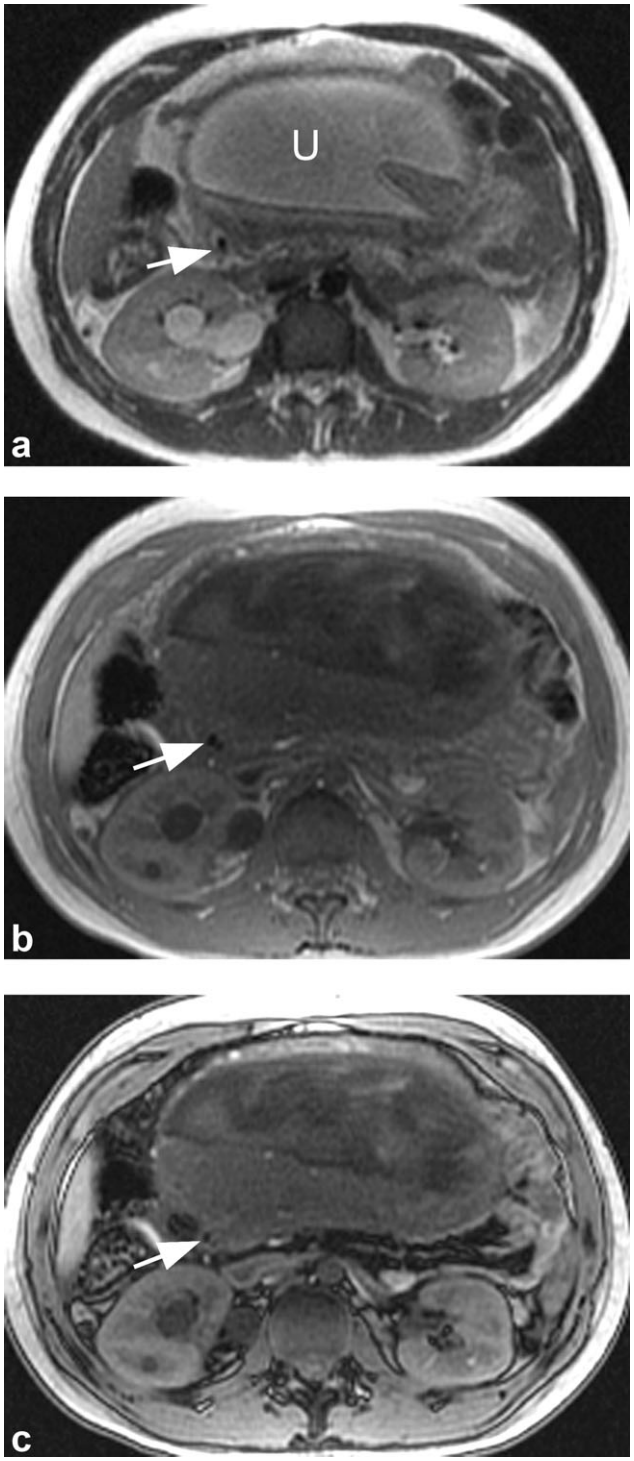

Figure 7. a–c: Axial T2-weighted SSFSE image (a) of a 21-year-old woman at 24 weeks gestational age with right-sided abdominal pain shows an appendicolith in the base of a fluid-filled, distended appendix (arrow) located behind the gravid uterus (U). Note better delineation of two adjacent appendicoliths in the T1-weighted gradient echo in-phase image (b, arrow) compared to the out-of-phase image (c, arrow) due to the longer echo time in the former, allowing for blooming of the calcified appendoliths. Acute appendicitis with appendicoliths was confirmed at surgery.

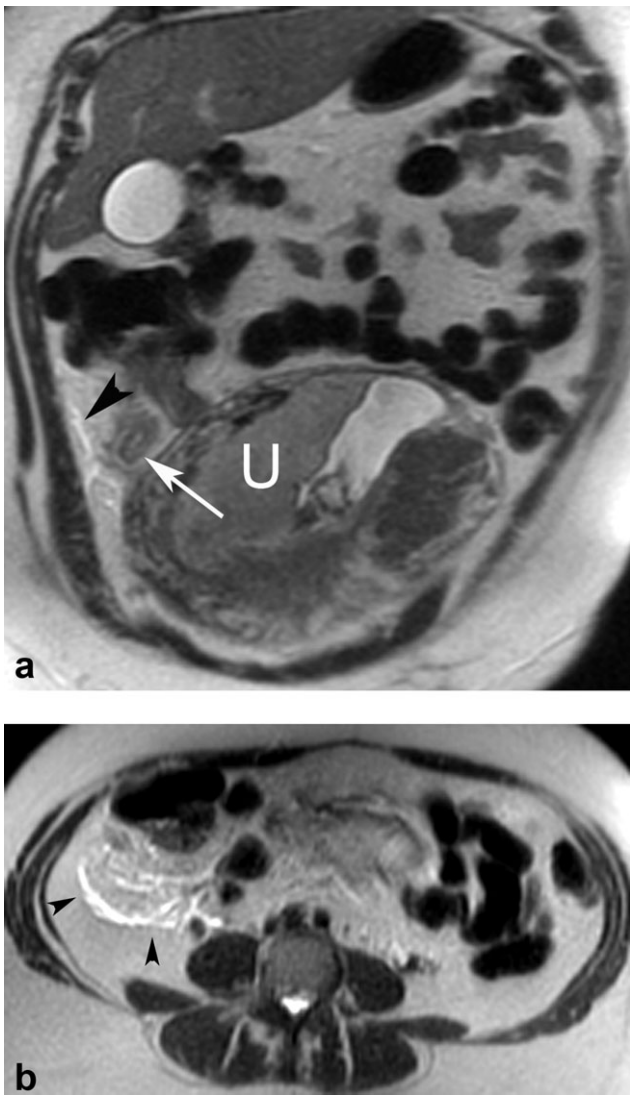

Figure 8. Coronal **(a)** and axial **(b)** T2-weighted SSFSE images of a 31-year-old woman at 19 weeks gestational age with acute right lower quadrant pain demonstrating a dilated appendix (arrow) with thin linear high-signal intensity bands (arrowheads) in the periappendiceal fat consistent with inflammation (arrow). Acute appendicitis was confirmed at surgery and histopathology.

Visualization rates for the normal appendix on MRI range from 86%–90% in the nongravid state to 87%–89% in pregnant patients (12,30,31), Identifying the appendix is extremely important, as a normal appendix on MRI virtually excludes acute appendicitis as a cause for abdominal pain with a reported negative predictive value of 100% (20). Identification of the appendix in the later stages of pregnancy can be challenging due to alterations in anatomy from the enlarging gravid uterus (Fig. 4). While the appendix can be superiorly displaced, there is only a moderate correlation between gestational age and the anatomic level of the appendix (32).

Lee et al (32) previously described the cecal tilt angle to localize the appendix on MRI. While the authors do not measure the cecal tilt angle routinely, it is helpful to assess the general orientation of the cecum as it facilitates finding the normal appendix. A cecal tilt angle of >90° (ie, tip of the cecum pointing anteriorly and superiorly relative to the inflexion point) is predictive of an appendiceal base level above the level of the fourth lumbar vertebral body with a specificity of 98% (32) (Fig. 3a,b).

ACUTE APPENDICITIS

The inflamed appendix is thickened, usually >7 mm in diameter (ie, outer wall-to-outer wall) on SSFSE sequences containing high-signal-intensity fluid within the lumen on T2-weighted imaging and frequently with peri-appendiceal fat stranding (Figs. 5,6) (10–13,27,31). As the material within the appendiceal lumen becomes more purulent, its signal intensity on the T2-weighted imaging can decrease, although the characteristic large appendiceal diameter in purulent appendicitis makes the diagnosis unequivocal.

Appendicoliths will appear as low signal intensity rounded structures on all imaging sequences. Appendicoliths can mimic the appearance of air; however, when combined with dilatation of the appendix distally appendiceal obstruction can be implied (27). Axial T1-weighted in- and out-phase GRE images are useful in demonstrating blooming from a calcified appendicolith (Fig. 7a–c).

An appendix that measures 6–7 mm without evidence of oral contrast material or air in its lumen is considered an indeterminate finding; in these cases, ancillary findings (eg, periappendiceal fat stranding, presence of phlegmon, abscess, and cecal wall thickening) are helpful in confirming the diagnosis of appendicitis. Periappendiceal fat stranding may be identified as thin linear bands of high-signal-intensity fluid on T2-weighted imaging and are supportive of the diagnosis (Fig. 8). Periappendiceal inflammatory change is often more prominent on fat-saturated T2-weighted sequences. In early cases of acute appendicitis the presence of periappendiceal edema can precede luminal dilatation and appendiceal wall thickening (27). A phlegmon can present on MRI as an ill-defined mass of heterogeneous moderate to high signal intensity on T2-weighted imaging (19,27,33). Subsequent abscess formation appears as a well-demarcated periappendiceal fluid collection that is of high signal on T2-weighted imaging. (27,33). Wall thickening of the cecum can also be seen in conjunction with acute appendicitis (34). A small amount of free fluid in the pelvis and/or paracolic gutters can be a normal finding during pregnancy and is not a helpful diagnostic clue. On DWI, the inflamed appendix demonstrates restricted diffusion and this can increase the conspicuity of the abnormal appendix (Fig. 9). A recent study assessing the efficacy of DWI in diagnosing acute appendicitis in nonpregnant patients showed a positive predictive value of 98.7% and a negative predictive value of 100% (26).

IMPACT OF MRI ON SURGICAL OUTCOMES

The sensitivity of MRI for diagnosing acute appendicitis has been reported from 90%–100% with a specificity of 94%–98% (19,27). Despite the excellent

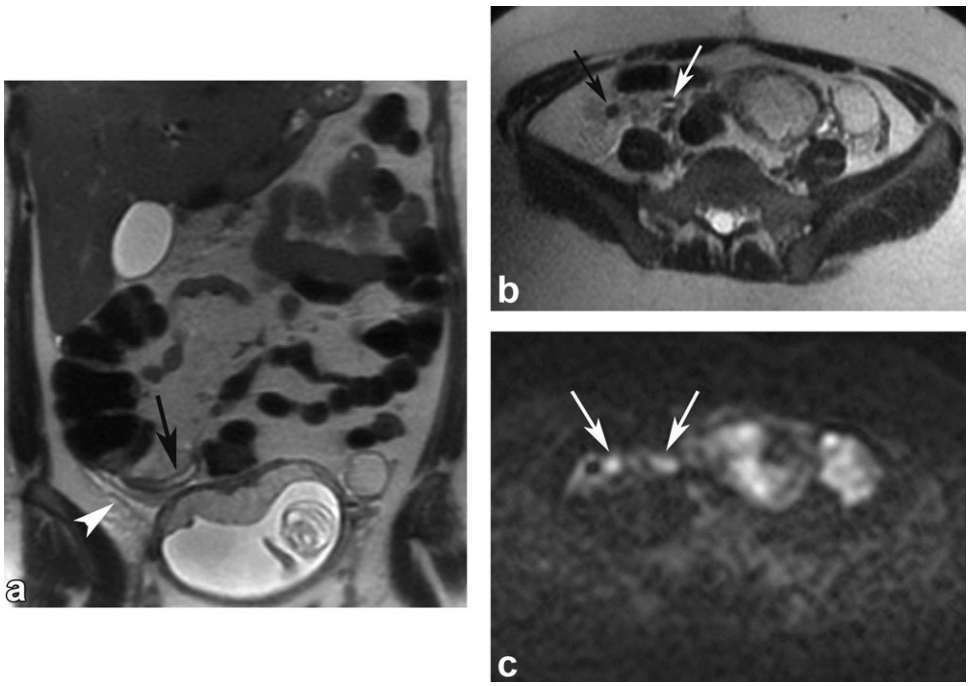

Figure 9. A 30-year-old woman at 15 weeks gestational age with right lower quadrant abdominal pain. Coronal T2-weighted SSFSE image **(a)** shows a mildly distended, fluid-filled appendix (arrow) with periappendiceal inflammation (arrowhead). Axial T2-weighted SSFSE (b) confirms these findings and shows greater degree of distension of the distal (ie, tip) aspect of the appendix (white arrow) relative to the base (black arrow). Axial DWI image (c) at the same level demonstrates marked hyperintensity in the inflamed appendix. Perforated appendicitis was confirmed at histopathology after laparoscopic appendectomy.

performance of MRI, a study in 2007 of academic institutions in the United States found that CT was preferred to MRI in assessing suspected appendicitis in the second and third trimester (35). Some of the bias towards CT may be related to out-of-hour's access to MRI and the complexity, length, and cost of MRI examinations. Some of these impediments may prevent the more widespread use of MRI in the acute setting, although practices may change in the near future with the increased awareness among physicians and the public about the potential risks of radiation exposure (36).

Table 2
Differential Diagnosis of Nonobstetrical Causes of Acute Abdominal Pain in Pregnancy

Nonobstetrical	Obstetrical
Surgical[a]	Labor
Acute appendicitis	Preterm labor
Adnexal torsion	Abruptio placenta
Ectopic/heterotopic pregnancy	Round ligament pain
	Chorioamnionitis
Nonsurgical[b]	Uterine rupture
Urological	
Urinary calculi	
Urinary Tract Infection/Pyelonephritis	
Gastrointestinal	
Cholecystitis	
Inflammatory bowel disease	
Pancreatitis	
Bowel obstruction	
Gastritis	
Mesenteric adenitis	
Gynecological	
Degenerating fibroids	
Adnexal mass	
Pelvic inflammatory disease	
Other	
Domestic violence	

[a]Commonly treated with surgery.
[b]Most frequently managed nonsurgically.

Negative laparotomy rates (NLR) and perforation rates (PR) are commonly accepted outcome indicators in the setting of clinically suspected acute appendicitis. Prior to the advent of radiological imaging, an NLR of 20% was accepted in nonpregnant patients, to avoid a high PR (37,38). However, in the pregnant population, given the risk to the fetus from high mortality associated with maternal appendiceal perforation, previously published NLR are as high as 25%–50% with PR varying around 22%–57% (8,9,39).

US has had variable results in the diagnosis of appendicitis in pregnancy with a negative predictive value of a nonvisualized appendix at best of 90% (14). At US only 2% of normal appendices are visualized compared to 87% at MRI (20). It was seen that CT had a favorable effect on the NLR without increasing the perforation rate, particularly in this patient population, although the radiation exposure and risk to the fetus was undesirable (39–42). The authors have previously documented an NLR of 30% with MRI in pregnant patients (20), which was higher than the rate achieved by Balthazar et al (39) of 8.3% using CT in nonpregnant patients of childbearing age. However, if

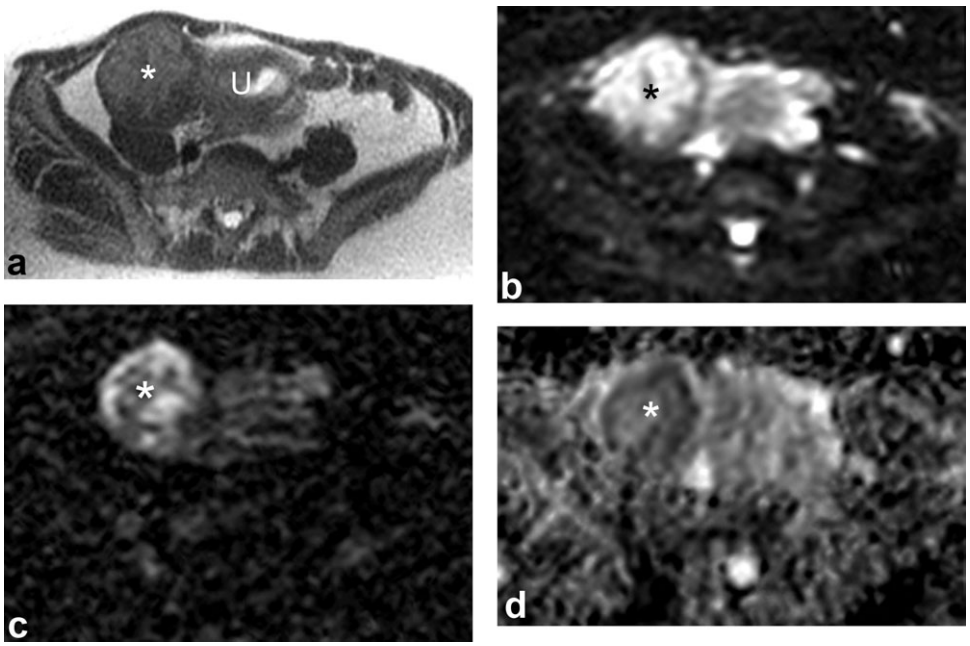

Figure 10. A 35-year-old woman at 15 weeks gestational age presenting with acute lower abdominal pain. Axial T2-weighted SSFSE image **(a)** of the pelvis demonstrates a large mass (asterisk) arising from the lateral aspect of the uterus (U) demonstrating diffuse mild increased signal intensity compared to that of skeletal muscle. Axial DWI images obtained with b = 0 **(b)** and b = 1000 **(c)** and corresponding ADC map **(d)** demonstrates marked restricted diffusion in the fibroid, consistent with acute degeneration.

the decision for surgery was based on negative MRI findings, then the adjusted NLR in that study would have been 7%, which is similar to other published studies (12,39). Indeed, in the authors' experience the visualization of a normal appendix at MRI virtually excludes the diagnosis of acute appendicitis. Also, the perforation rate of 21% was similar to the 19% reported by Balthazar et al (39) and more favorable than other studies (12).

DIFFERENTIAL DIAGNOSIS

There is a broad range of conditions causing abdominal pain in pregnancy, as outlined in Table 2 (43). The main gynecological surgical emergencies that must be excluded include ectopic pregnancy and ovarian torsion. In ectopic pregnancy, MRI is useful if US imaging is inconclusive, the clinical suspicion is high, and a prompt diagnosis is required (44,45). The MRI findings in ovarian torsion can vary depending

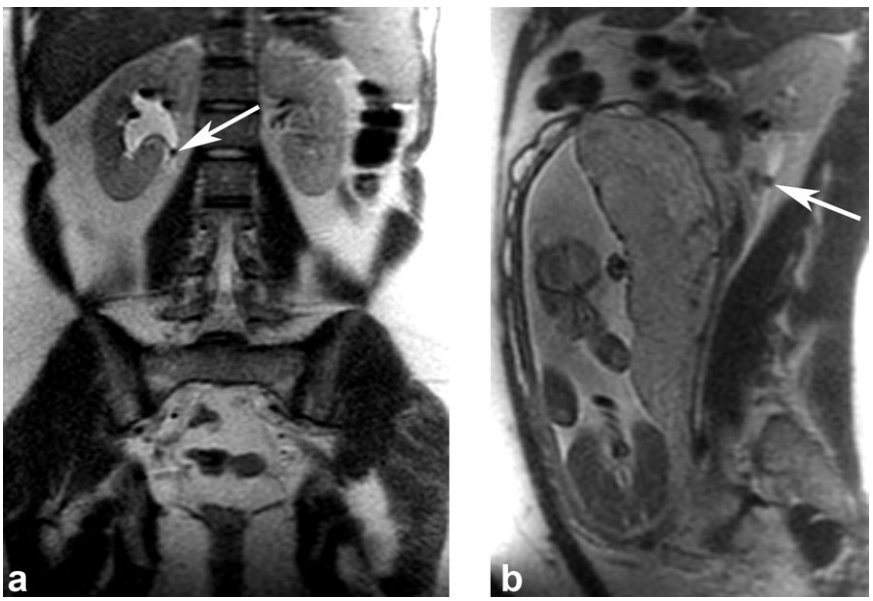

Figure 11. Coronal **(a)** and sagittal **(b)** SSFSE of a 25-year-old woman at 32 weeks gestation and right-sided abdominal pain showing persistent filling defect in the proximal right ureter consistent with a stone (arrow).

on the stage of the disease. Initially, there is ovarian enlargement secondary to stromal edema, which is appreciated by diffuse high signal intensity on T2-weighted imaging. Fat-saturation sequences improve the detection of edema on T2-weighted imaging. As ovarian torsion progresses the signal intensity may change due to the presence of hemorrhage and necrosis. Decreased signal on both T1- and T2-weighted imaging indicates hemorrhagic infarction. Other ancillary findings include tubal thickening, increased signal intensity on T2-weighted imaging within the fallopian tube, deviation of the uterus to the side of the torsion, and a twisted vascular pedicle (46,47).

Leiomyomas can enlarge during pregnancy and if they outgrow their blood supply can degenerate. Red degeneration, a hemorrhagic infarction that occurs secondary to venous thrombosis, is the most common subtype of degeneration occurring during pregnancy. However, in the authors' experience pregnant patients presenting with an acute onset of abdominal pain related to fibroid degeneration usually exhibit diffuse edema of the fibroid prior to the development of frank necrosis. At this stage, uterine leiomyomas demonstrate diffuse high signal intensity on T2-weighted images and a characteristic restricted diffusion on DWI (Fig. 10). Diffuse or peripheral high signal on T1-weighted imaging and variable signal on T2-weighted imaging are typically present in leiomyomas undergoing frank hemorrhagic degeneration (48–50). Fibroid degeneration as the cause of abdominal pain is usually a diagnosis of exclusion in patients with no other cause identified and obvious findings on MRI. Occasionally, identification and compression of the fibroid with a US probe can replicate the pain and confirm this diagnosis.

Pathological processes involving the gastrointestinal tract in pregnancy include primarily inflammatory bowel disease, diverticulitis, and obstruction. MRI allows exquisite visualization of the small and large bowel. Bowel wall edema is best appreciated on FS T2-weighted SSFSE images as a band of increased signal intensity within the thickened wall. Complications of bowel inflammation including fistulas and abscesses can be accurately seen at MRI (51,52). SSFSE images have shown excellent sensitivity for detection of bowel obstruction and demonstrate the cause of the obstruction in ~50% of these patients (53)

The utility of MRI in detecting nephro- and ureterolithiasis has been reported in nonpregnant and pregnant patients using T2-weighted half-Fourier SSFSE sequences (54–56). Hydronephrosis related to pregnancy can be readily recognized, as the gravid uterus is seen to compress the ureter against the psoas muscle posteriorly at the level of the sacral promontory. Ureteral stones are recognized on SSFSE images as filling defects of low signal intensity. Care should be taken to ensure that flow in the ureter is not mistaken for a calculus on T2-weighted SSFSE images; flow-related filling defects within the ureter do not persist on different imaging planes, whereas real stones persist in multiple acquisitions (Fig. 11). Fast imaging with a steady-state precession technique (eg, true FISP [Siemens Medical Solutions, Malvern, PA], FIESTA [GE Healthcare, Waukesha, WI], or balanced FFE [Philips Medical System, Andover, MA]) may be used to identify calculi in the distal ureter. A 3D version of a steady-state precession sequence allows improved signal-to-noise ratio, thinner slices, and multiplanar reformations to facilitate recognition of the stone.

CONCLUSION

Identification of the appendix, whether healthy or inflamed, is crucial in the clinical management of pregnant patients with suspected acute appendicitis. MRI is an extremely sensitive test for acute appendicitis and visualization of the normal appendix virtually excludes acute appendicitis. The technique described is relatively simple and reliable and provides a systematic evaluation of the entire abdomen and pelvis, enabling imaging of a wide range of differential diagnoses.

REFERENCES

1. Mourad J, Elliott J, Erickson L, et al. Appendicitis in pregnancy: new information that contradicts long-held clinical beliefs. Am J Obstet Gynecol 2000;182:1027–1029.
2. Mazze RI, Kallen B. Appendectomy during pregnancy: a Swedish registry study of 778 cases. Obstet Gynecol 1991;77:835–840.
3. Gilo NB, Amini D, Landy HJ. Appendicitis and cholecystitis in pregnancy. Clin Obstet Gynecol 2009;52:586–596.
4. Anderson B, Nielson TF. Appendicitis in pregnancy: diagnosis, management and complications. Acta Obstet Gynecol Scand 1999;78:758–762.
5. Cappell MS, Friedel D. Abdominal pain during pregnancy. Gastroenterol Clin North Am 2003;32:1–58.
6. McCollough CH, Schueler BA, Atwell TD, et al. Radiation exposure and pregnancy: when should we be concerned? Radiographics 2007;27:909–917.
7. ACOG Committee on Obstetric Practice. ACOG Committee opinion number 299, September 2004 — guidelines for diagnostic imaging during pregnancy. Obstet Gynecol 2004;104:647–651.
8. McGory ML, Zingmond DS, Tillou A, et al. Negative appendicectomy in pregnant women is associated with a substantial risk of fetal loss. J Am Coll Surg 2007;205:534–540.
9. Tracey M, Fletcher HS. Appendicitis in pregnancy. Am Surg 2000;66:555–559; discussion 559–560.
10. Cobben LP, Groot I, Haans L, et al. MRI for clinically suspected appendicitis during pregnancy. AJR Am J Roentgenol 2004;183:671–675.
11. Birchard KR, Brown MA, Hyslop WB, et al. MRI of acute abdominal and pelvic pain in pregnant patients. AJR Am J Roentgenol 2005;184:452–458.
12. Oto A, Ernst RD, Shah R, et al. Right-lower-quadrant pain and suspected appendicitis in pregnant women: evaluation with MR imaging—initial experience. Radiology 2005;234:445–451.
13. Pedrosa I, Levine D, Eyvazzadeh AD, et al. MR imaging evaluation of acute appendicitis in pregnancy. Radiology 2006;238:891–899.
14. Lim HK, Bae SH, Geo GS. Diagnosis of acute appendicitis in pregnant women: value of sonography. AJR Am J Roentgenol 1992;159:539–542.
15. Puylaert JB. Acute appendicitis: US evaluation using graded compression. Radiology 1986;158:355–360.
16. Kanal E, Borgstede JP, Barkovich AJ, et al. American College of Radiology white paper on MR safety. AJR Am J Roentgenol 2002; 178:1335–1347.
17. Cobben LP, Groot I, Haans L, et al. MRI for clinically suspected appendicitis during pregnancy. AJR Am J Roentgenol 2004;183: 671–675.
18. Israel GM, Malguria N, McCarthy S, et al. MRI vs. ultrasound for suspected appendicitis in pregnancy. J Magn Reson Imaging 2008;28:428–433.
19. Singh AK, Desai H, Novelline RA. Emergency MRI of acute pelvic pain: MR protocol with no oral contrast. Emerg Radiol 2009;16:133–141.
20. Pedrosa I, Lafornara M, Pandharipande, et al. Pregnant patients suspected of having acute appendicitis: effect of MR imaging on

negative laparotomy rate and appendiceal perforation rate. Radiology 2009;250:749–757.
21. Shellock FG, Kanal E. Safety of magnetic resonance imaging contrast agents. J Magn Reson Imaging 1999;10:477–484.
22. Regan F, Beall DP, Bohlman ME, et al. Fast MR imaging and the detection of small-bowel obstruction. AJR Am J Roentgenol 1998; 170:1465–1469.
23. Webb JAW, Thomsen HS, Morcos SK. The use of iodinated and gadolinium contrast media during pregnancy and lactation. Eur Radiol 2005: 15:1234–1240.
24. Rosenkrantz A, Oei M, Babb J, et al. Diffusion-weighted imaging of the abdomen at 3.0T: image quality and apparent diffusion coefficient reproducibility compared with 1.5T. J Magn Reson Imaging 2011;33:128–135.
25. Theony H, Binser T, Roth B, et al. Non-invasive assessment of acute ureteral obstruction with diffusion-weighted MR imaging. Radiology 2009;252:721–728.
26. Inci E, Kilickesmesz O, Hocaoglu E, et al. Utility of diffusion imaging in the diagnosis of acute appendicitis. Eur J Radiol 2011;21:768–775.
27. Pedrosa I, Rofsky NM. MR imaging in abdominal emergencies. Radiol Clin North Am 2003;41:1243–1273.
28. Patel S, Reede DL, Katz DS, et al. Imaging the pregnant patient for non-obstetric conditions: algorithms and radiation dose considerations. Radiographics 2007;27:1705–1722.
29. Birnbaum BA, Wilson SR, et al. Appendicitis at the millennium. Radiology 2000;215:337–348.
30. Nitta N, Furukawa A, et al. MR imaging of the normal appendix and acute appendicitis. J Magn Reson Imaging 2005;21:156–165.
31. Hormann M, Puig S, Prokesch SR, et al. MR imaging of the normal appendix in children. Eur J Radiol 2002;12:2313–2316.
32. Lee KS, Rofsky NM, Pedrosa I. Localization of the appendix at MR imaging during pregnancy: utility of the cecal tilt angle. Radiology 2008;249:134–141.
33. Incesu L, Coskun A, Selchek MB, et al. Acute appendicitis: MR imaging and sonographic correlation. AJR Am J Roentgenol 1997;168:669–674.
34. Eyvazzadeh AD, Pedrosa I, Rofsky NM, et al. MRI of right-sided abdominal pain in pregnancy. AJR Am J Roentgenol 2004;183: 907–914.
35. Jaffe TA, Miller CM, Merkle EM. Practice patterns in imaging of the pregnant patient with abdominal pain: a survey of academic centers. AJR Am J Roentgenol 2007;189:1128–1134.
36. Kilpatrick CC, Orejuela FJ. Management of the acute abdomen in pregnancy: a review. Curr Opin Obstet Gynecol 2008;20:534–539.
37. Velanovich V, Satava R. Balancing the normal appendicectomy rate with the perforated appendicitis rate: implications for quality assurance. Am J Surg 1992;58:264–269.
38. Berry J Jr, Malt RA. Appendicitis near its century. Ann Surg 1984;200:567–575.
39. Balthazar EJ, Rofsky NM, Zucker R. Appendicitis: the impact of computed tomography imaging on negative appendectomy and perforation rates. Am J Gastroenterol 1998;93:768–771.
40. Bendeck SE, Nino-Murcia M, Berry GJ, et al. Imaging for suspected appendicitis: negative appendicectomy and perforation rates. Radiology 2002;225:1131–1136.
41. Togowa A, Kimura F, Chiku T, et al. Simple way to improve accuracy in diagnosis of quadrant inflammatory disease: how to avoid adverse laparotomy by using plain CT. Hepatogastroenterology 2005;52:135–138.
42. Wallace CA, Petrov MS, Soybel DI, et al. Influence of imaging on the negative appendectomy rate in pregnancy. J Gastroenterol Surg 2008;12:46–50.
43. Beddy P, Griffen N, Keogan M, Sala E. Magnetic resonance imaging of acute abdominal pain in pregnancy. Semin Ultrasound CT MR 2010;31:433–434.
44. Barnhart KT, Sammel MD, Gracia CR, et al. Risk factors for ectopic pregnancy in women with symptomatic first-trimester pregnancies. Fertil Steril 2006;86:36–43.
45. Lozeau AM, Potter B. Diagnosis and management of ectopic pregnancy. Am Fam Physician 2005;72:1707–1714.
46. Rha SE, Byun JY, Jung SE, et al. CT and MR imaging features of adnexal torsion. Radiographics 2002;22:283–294.
47. Kimura I, Togashi K, Kawakami S, et al. Ovarian torsion: CT and MR imaging appearances. Radiology 1994;190:337–341.
48. Strobelt N, Ghidini A, Cavallone M, et al. Natural history of uterine leiomyomas in pregnancy. J Ultrasound Med 1994;13: 399–401.
49. Ouyang DW, Economy KE, Norwitz ER. Obstetric complications of fibroids. Obstet Gynecol Clin North Am 2006;33:153–169.
50. Murase E, Siegalman ES, Outwater EK, et al. Uterine leiomyomas: histopathologic features, MR Imaging findings, differential diagnosis, and treatment. Radiographics 1999;19:1179–1197.
51. Fidler JL, Guimaraes L, Einstein DM. MR imaging of the small bowel. Radiographics 2009;29:1811–1825.
52. Siddiki HA, Fidler JL, Fletcher JG, et al. Prospective comparison of state-of-the-art MR enterography and CT enterography in small bowel Crohn's disease. AJR Am J Roentgenol 2009;193: 113–121.
53. Regan F, Beall DP, Bohlman ME, Khazan R, Sufi A, Schaefer DC. Fast MR imaging and the detection of small-bowel obstruction. AJR Am J Roentgenol 1998;170:1465–1469.
54. Tang Y, Yamashita Y, Namimoto T, et al. The value of MR urography that uses HASTE sequences to reveal urinary tract disorders. AJR Am J Roentgenol 1996;167:1497–1502.
55. Regan F, Petronis J, Bohlman M, et al. Perirrenal MR high signal: a new and sensitive indicator of acute ureteric obstruction. Clin Radiol 1997;52:445–450.
56. Roy C, Saussine C, Jahn C, et al. Fast imaging MR assessment of ureterohydronephrosis during pregnancy. Magn Reson Imaging 1995;13:767–772.